Glassy behaviour in simple kinetically constrained models: topological networks, lattice analogues and annihilation-diffusion

2002 J. Phys.: Condens. Matter 14 1673

(http://iopscience.iop.org/0953-8984/14/7/323)

INSTITUTE OF PHYSICS PUBLISHING JOURNAL OF PHYSICS: CONDENSED MATTER

J. Phys.: Condens. Matter **14** (2002) 1673–1682 PII: S0953-8984(02)31467-X

Glassy behaviour in simple kinetically constrained models: topological networks, lattice analogues and annihilation–diffusion

David Sherrington, Lexie Davison, Arnaud Buhot and Juan P Garrahan

Department of Physics, Theoretical Physics, University of Oxford, 1 Keble Road, Oxford OX1 3NP, UK

Received 3 December 2001
Published 7 February 2002
Online at stacks.iop.org/JPhysCM/14/1673

Abstract

We report a study of a series of simple model systems with only non-interacting Hamiltonians, and hence simple equilibrium thermodynamics, but with constrained dynamics of a type initially suggested by foams and idealized covalent glasses. We demonstrate that macroscopic dynamical features characteristic of real and more complex model glasses, such as two-time decays in energy and auto-correlation functions, arise from the dynamics and we explain them qualitatively and quantitatively in terms of annihilation–diffusion concepts and theory. The comparison is with strong glasses. We also consider fluctuation-dissipation relations and demonstrate subtleties of interpretation. We find no FDT breakdown when the correct normalization is chosen.

1. Introduction

Glasses are amorphous solid-like systems, produced when liquids are supercooled at a rate which is too fast to permit equilibration. They are characterized by a combination of fast and slow temporal evolution; for example by correlation and response functions having a fast initial (β) decay, followed by a plateau and then a slow (α) decay whose effective onset becomes later and slower either with lower temperature in an already equilibrated (or quasi-equilibrated) system or as a function of the time since its quench (from the liquid state) in a non-equilibrated scenario. Conventional real glasses have interactions between their atoms or molecules, but in this paper we show that such behaviour occurs due to purely kinetic constraints in some simple many-body systems with non-interacting Hamiltonians.

We follow a minimalist philosophy, progressing from topological foam-like networks to simple lattice-based analogues and relate our observations to novel annihilation–diffusion processes. Although initially inspired by foams, our basic model can also be related to an idealized covalently bonded system and indeed the behaviour which results has the Arrhenius relaxation-time behaviour characteristic of strong glasses (in the nomenclature of Angell [1]),

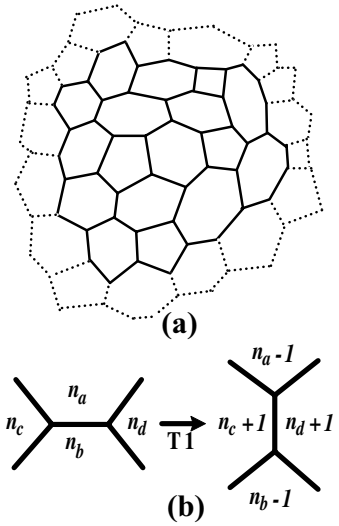

Figure 1. (a) A topologically stable cellular partition (froth). (b) A T1 move (from [2]).

whose examples are typically covalent. After recognition of the underlying conceptual consequences, the models can be further simplified and extended.

2. Topological network models

The first model we consider [2, 3] is based on the topology of a foam; i.e. it is characterized by a fully connected network of three-armed vertices, as shown in figure 1(a). By Euler's theorem, the average number of edges per cell is six. The crystalline form is hexagonal. To ensure the latter as ground state in a minimalist manner, we choose an energy function

$$E = \sum_{i=1}^{N} (6 - n_i)^2 \tag{1}$$

where $i = 1 \ldots N$ labels the cells, and n_i refers to the number of sides of cell i. Clearly such a model has trivial thermodynamics and no finite temperature phase transition. The interest comes from the dynamics. Again we choose as simply as possible, permitting only T1 moves as illustrated in figure 1(b); these conserve the total number of cells, edges and vertices. Thermal effects are introduced by making the T1 moves stochastic with acceptance probabilities determined by $\mathrm{Min}[1, \exp(-\Delta E/T)]$, where ΔE is the energy change which would ensue. To avoid unphysical features, moves which would produce two-sided or self-neighbouring cells are forbidden.

This model can also be related to an idealization of a two-dimensional covalently bonded glass, for which the vertices of figure 1(a) are sp^2 hybrids and the edges are the covalent bonds. The preferred angle between the sp^2 lobes is $2\pi/3$ and, in a harmonic approximation which ignores correlations, a perturbation to an angle θ costs an energy $\sim(\theta - 2\pi/3)^2$. If we further take θ to have the average value $(4\pi/n)$ in a cell of n sides, there results an approximate energy

$$H \sim \sum_{i=1}^{N} (6 - n_i)^2/(6n_i)^2 \tag{2}$$

which can be further approximated by (1).

Simulations [2,3] show that the system equilibrates easily at high temperatures (the 'liquid state') but below a temperature of order unity (in the above units) it exhibits glassy behaviour of the type discussed in the introduction.

Rather than discussing this behaviour in detail here, we note that it can be understood in terms of a picture of annihilating and diffusing defects. These defects are cells which deviate from the ground state values $n_i = 6$, i.e. of non-zero topological charge $q_i = (6 - n_i)$. A T1 process increases the topological charges on each of the initially adjacent cells and decreases the charges on the other two cells (which become adjacent). By so doing it provides mechanisms of defect annihilation, creation and diffusion. At low temperatures only $q = \pm 1, 0$ are present in significant numbers and henceforth we restrict consideration to these (but generalization is easy). A brief consideration then convinces one that: (i) energy reduction is only possible through the annihilation of a pair of adjacent oppositely charged topological charges, i.e. a dimer, in a process in which the other two cells either have appropriately opposite charges or one a non-zero and the other a zero charge; (ii) a pair of adjacent opposite charges in a zero background can move without energy cost, given the appropriate T1 move, and (iii) an isolated non-zero charge can move only by increasing the overall energy, metamorphosing into three non-zero charges on neighbouring sites, two of the same sign and one opposite to that originally present. Since no energy cost is involved the first two of these processes can occur even at zero temperature with the microscopic timescale, while the third is activated with a timescale of Arrhenius form.

Although we could pursue this A, B annihilation–diffusion image further at this stage we believe it to be more productive to use it first to pass to lattice analogues which can be simulated more easily on larger systems for longer times.

3. Lattice models

3.1. Hexagonal lattice

A simple lattice analogue of the topological foam [4] consists of a set of 3-state spins $s_i = 0, \pm 1$ on the cells of a hexagonal lattice, with energy function

$$E = D \sum_{i=1}^{N} s_i^2 \tag{3}$$

and $\sum_i s_i = 0$ to emulate Euler's theorem. As an analogue of a T1 process we pick an edge on the hexagonal lattice and randomly increase (decrease) by one the spins on the adjacent cells and decrease (increase) by one those on the cells at its ends; see figure 2. As before, these moves are executed stochastically with an acceptance probability determined by $\mathrm{Min}[1, \exp(-\Delta E/T)]$, with moves which would place a spin outside the range $0, \pm 1$ forbidden.

The original topological foam model is emulated by $D > 0$, for which the ground state is unique, but it is straightforward to extend our study to $D < 0$ for which the ground state is highly degenerate (± 1 on any site, independently of the others).

3.1.1. $D > 0$. Figure 3 shows results of simulations together with theoretically inspired fits, to be explained below, respectively for: (a) the energy as a function of time for a system started from a random high-temperature state but evolving with Metropolis–Kawasaki dynamics corresponding to a range of low temperatures, (b) the autocorrelation

$$C(t_w, t_w + t) = \frac{\sum_{i=1}^{N} s_i(t_w) s_i(t_w + t)}{\sum_{i=1}^{N} s_i^2(t_w)} \tag{4}$$

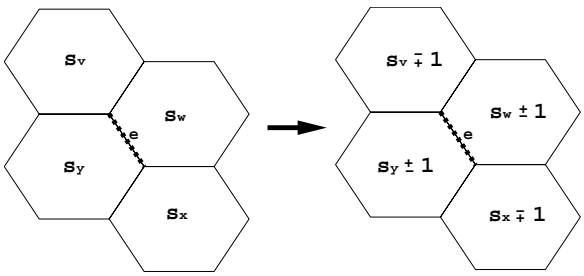

Figure 2. The analogue of a T1 move for the hexagonal lattice model.

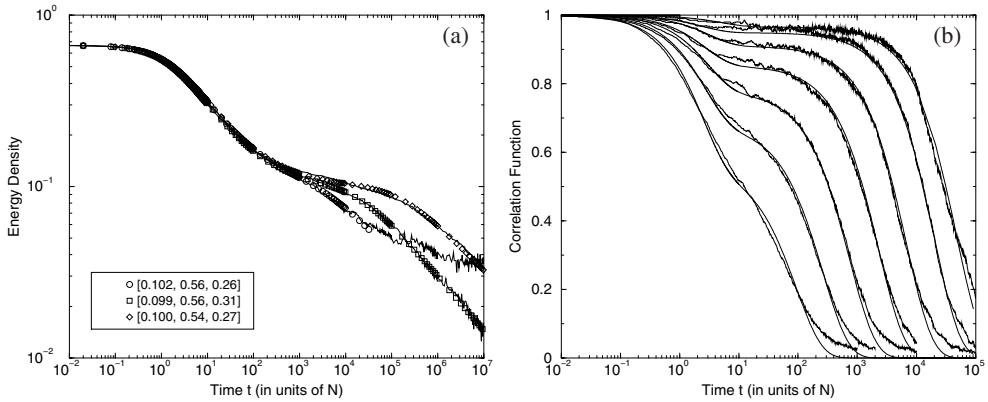

Figure 3. (a) The energy density E/N of the hexagonal system with $D > 0$ as a function of time after the quench for inverse temperatures $\beta = 4, 5, 6$ (from left to right), fitted with equation (8). (b) The equilibrium auto-correlation function as a function of time for, from left to right, $\beta = 3, 3.5, 4, 4.5, 5, 5.5, 6$. The solid curves superimposed are fits of the form of (9).

for systems at various temperatures and in equilibrium (so that there is no dependence on t_w). In both cases one has an initial rapid decay, followed by a plateau and then a slow temperature-dependent decay. As figure 3(a) shows clearly, the timescale of the initial decay is not temperature dependent.

These results can be understood in terms of an annihilation–diffusion model, with the s_i playing the role of the topological charges in the earlier discussion. Thus, we can consider $s = 0, \pm 1$ as $\emptyset$, A, B. Annihilation involves

$$2A + 2B \to \emptyset \tag{5a}$$

$$2A + B \to A \qquad A + 2B \to B \tag{5b}$$

over sets of four sites as in figure 2, with (5b) statistically more probable than (5a). Fast diffusion can only occur for neighbouring AB dimers. These are the processes which drive the initial decays in figure 3. To further understand the approach to and the magnitude of the plateau in $E(t)$ note that at $t = 0$ the system has a defect distribution corresponding to infinite temperature (1/3 each of 0, +1, −1), while at the plateau essentially all the (+1, −1) neighbouring pairs have been eliminated by the above processes; actually at finite temperature there remain some due to thermal excitation but they are negligible on the scale shown. The initial decay in $C(t)$ is also due to dimer diffusion, since movement of a spin alters its autocorrelation, reducing C, but the total dimer density remains unchanged since the system remains in equilibrium.

The second slower decays require the motion of isolated defects (± 1 spins). For $C(t)$ the motion itself is sufficient to affect the value, whereas for $E(t)$ the defects must pair up as $(+\,-)$ dimers which then diffuse quickly and annihilate. Since the dimer diffusion is much faster than that of the isolated defects we can effectively consider it as instantaneous on the timescale of the isolated defects. We are therefore left with a picture of the slow process as also one involving effective $\tilde{A}$, $\tilde{B}$ particles diffusing with a much slower timescale and annihilating via

$$\tilde{A} + \tilde{B} \to \emptyset. \tag{6}$$

We are now in a position to utilize results from the field theory of annihilation–diffusion processes [5,6] to provide fits to the simulations. Considering $E(t)$ first, this can be related to the densities of particles in the usual annihilation–diffusion theory. Noting that (5b) dominates the fast annihilation and that the A and B concentrations remain equal due to $\sum s_i = 0$, then within mean-field theory these are expected to behave as

$$A + A + A \to A \tag{7}$$

and to give the first (fast) energy decay as $(t/\tau_1)^{-1/2}$ where τ_1 is the microscopic time. Since the critical dimension for this process is 1 and we are in $d = 2$ we expect the mean-field result to hold. For the slow process we note that (6) yields a $(t/\tau_2)^{-d/4}$ standard asymptotic form, so here in $d = 2$ again we expect the exponent $-1/2$, but now with τ_2 scaling as $\exp(2\beta)$, where $\beta = T^{-1}$, since the energy needed to create a dimer to move an isolated defect is 2 (and, of course, correspondingly the number of thermal dimers, able to move an isolated defect by 'collisions', scales as $\exp(-2\beta)$). Taking account of the further fact that $\tau_1 = 2$, since only one of the two quasi-T1 moves is acceptable at any trial, we are left with the predicted form for $E(t)$:

$$\frac{E(t)}{N} = \left(\frac{2}{3} - a\right)\left(1 + \frac{t}{2}\right)^{-b} + (a - e_{\mathrm{eq}})\left(1 + \frac{t}{\mathrm{e}^{2\beta}}\right)^{-c} + e_{\mathrm{eq}} \tag{8}$$

where a is the plateau value, e_{eq} is the energy per spin in equilibrium and we expect both b and c to be close to 0.5. The fit values are shown in the key to figure 3(a) and are seen to be in very good accord with expectations. We have not calculated a from first principles but have checked that the value found is less than that which ensues from randomly removing dimers from an initial high-temperature configuration (which should be an upper bound).

As noted earlier, $C(t)$ is reduced by a move of a defect by even one step and does not require annihilation. Consequently we expect its dependence on t to involve two exponentials (for the two timescales) rather than power laws. Hence we fit to

$$C(t) = \alpha \mathrm{e}^{-t/\tau_1} + (1 - \alpha)\mathrm{e}^{-t/\tau_2} \tag{9}$$

again with $\tau_2 \sim \exp(B/T)$ and the expectation that $B \simeq 2$. Figure 3(b) shows the result with B in fact found to be about 2.12. The plateau value is somewhat more complicated. The initial fast decay of the correlation function is dominated by the initial configurations which can move freely but account must also be taken of oscillating-like pairs ((+1, +1) or $(-1, -1)$). Taking account of both effects leads to

$$\alpha(T) = \frac{12\exp(-\beta)}{1 + 2\mathrm{e}^{-\beta}} \tag{10}$$

which closely accords with the fits in figure 3(b).

3.1.2. $D < 0$. As noted, for $D > 0$ the ground state is highly degenerate. Nevertheless, $E(t)$ and $C(t)$ again have the same form of fast decay to a plateau followed by slow decay characterized by an Arrhenius timescale. There are, however, important differences of detail,

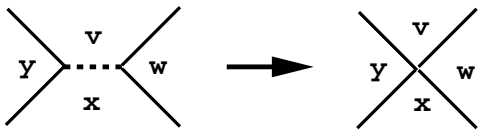

Figure 4. The square lattice (right) can be considered equivalent to a hexagonal lattice (left) in which the central bond, denoted by a dashed line, has been shrunk to a point.

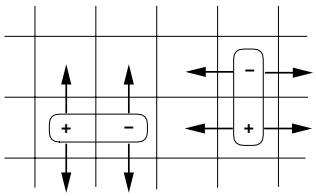

Figure 5. Dimer motion on a square lattice.

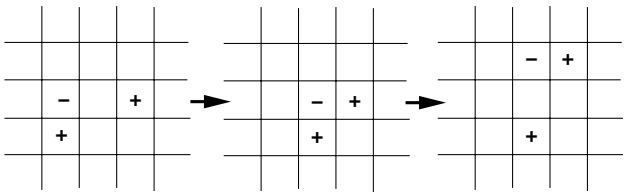

Figure 6. Singleton motion on a square lattice.

caused by the fact that there is now only a single defect type, 0, and also because the resultant dimers cannot move so easily through the ± 1 background. Because of the single type of defect the slower processes are now of the type

$$\tilde{A} + \tilde{A} \rightarrow \emptyset. \tag{11}$$

In a free background this would be expected to yield a decay as $(t/\tau_2)^{-d/2}$, but in fact a fit to $(t/\tau_2)^{-\kappa}$ yields $\kappa \sim 0.6$ due to the hindering of dimer motion by the $\pm$ ground state background. Similarly, in $C(t)$ the slow decay is better fit with a stretched exponential $\sim \exp(-(t/\tau_2)^{\gamma})$ with $\gamma \sim 0.8$.

3.2. Square lattice

Although the hexagonal lattice 'matches' the original topological foam model in its general structure and vertex character, the annihilation–diffusion picture does not require it. Hence it is interesting to simplify the model further, while hopefully retaining the fundamental essentials.

One natural simplification is to a square lattice [7], again with $s_i = 0, \pm 1$ associated with the cells. We replace the 'Feynman-diagram' T1 process by one involving four cells around a four-vertex, as illustrated in figure 4. Dimers are now constrained to move one-dimensionally (see figure 5), but the defects within them can still move two-dimensionally by switching partners (see figure 6). $E(t)$ and $C(t)$ still show the same characteristic behaviour (figure 7) and the annihilation–diffusion explanations continue to apply.

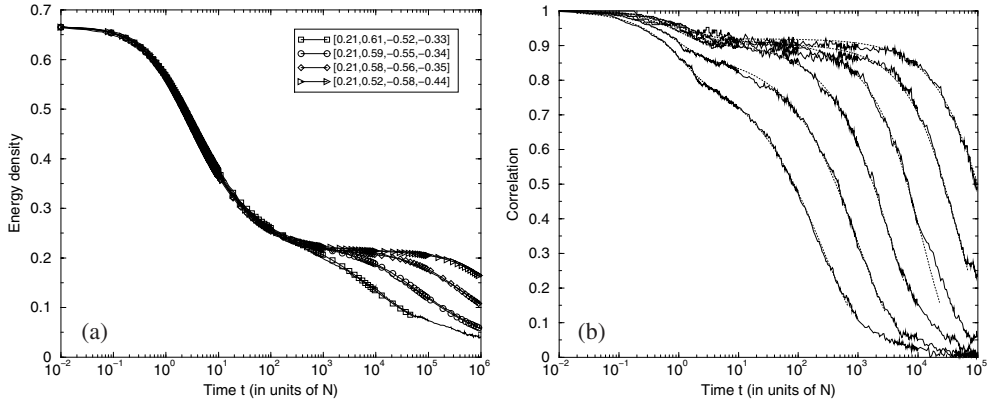

Figure 7. (a) The energy function of the square system fitted with $E/N = (\frac{2}{3} - a)(1+mt)^{\kappa_1} + a(1+te^{-2\beta})^{\kappa_2}$ for, from left to right, $\beta = 4, 5, 6, 7$. Values in the inset are for $[a, m, \kappa_1, \kappa_2]$. (b) The equilibrium correlation functions for, from left to right, $\beta = 3, 3.5, 4, 4.5, 5, 5.5$. The dotted lines are fits of the form $C(t) = \alpha e^{-t/\tau_1} + (1 - \alpha)e^{-(t/\tau_2)^{\gamma}}$.

3.3. Other dimensions

Other variants can and have been devised in several dimensions, showing the characteristic features through the combination of easy dimer diffusion, annihilation of dimers in three and four 'particle' interchanges, and Arrhenius-type slow singleton motion.

4. Fluctuation-dissipation

Another issue which has caused much interest in glass theory recently concerns deviations from the usual fluctuation-dissipation theorem (FDT) and their use to define an effective temperature in the glassy region. Hence it seems appropriate to consider the corresponding behaviour for the models under study here.

For a conventional system one considers the effect on the measurement of an operator A of switching on a conjugate field h; i.e. adding a Hamiltonian perturbation $-hA\theta(t - s)$ where $\theta(x)$ is the Heaviside unit function ($= 1$ for $x > 0$, $= 0$ for $x < 0$). Denoting the linear response susceptibility at t by $R_A(t, s)$ one may then write

$$R_A(t, s) = \beta X(t, s)[C_A(t, t) - C_A(t, s)] \tag{12}$$

where

$$C_A(t, s) = \langle A(t)A(s)\rangle - \langle A(t)\rangle\langle A(s)\rangle \tag{13}$$

with the expectations $\langle\,\rangle$ those for the unperturbed system. In equilibrium $C_A(t, s) = C_A(t-s)$ and $X(t, s) = 1$, giving the conventional FDT. However, out of equilibrium this needs possible modification. For many glassy systems it has been noted that

$$X(t, s) = x(C(t, s)) \tag{14}$$

and, furthermore, in the glassy region where $C(t, s)$ is less than its plateau value one finds

$$\beta X = T_{\text{eff}}^{-1} < T^{-1} \tag{15}$$

thereby defining an effective temperature in the glass of $T_{\text{eff}} > T$. For $C(t, s)$ greater than the plateau value $X(t, s) = 1$ and FDT is recovered. Parametric plots of the integrated response against the correlation function have demonstrated such an effective temperature in many

studies of $p(>2)$-spin glasses and structural glasses. Hence we consider the corresponding situation for our model.

Since we have been considering auto-correlation functions we also wish to consider auto-response. This can be achieved by the now-standard procedure of applying random field-signs to the different sites and corresponding signs to the responses, yielding auto-functions in the self-averaging $N \to \infty$ limit. Hence we take as perturbation

$$\Delta E(t) = -h \sum_{i=1}^{N} \epsilon_i s_i(t) \theta(t - t_w) \tag{16}$$

where the ϵ_i are chosen randomly ± 1 and quenched. Then the un-normalized response function that we measure is

$$\tilde{R}(t + t_w, t_w) = h^{-1} N^{-1} \sum_{i=1}^{N} \epsilon_i s_i(t + t_w) \equiv N^{-1} \sum_i \partial \langle s_i(t + t_w) \rangle / \partial h_i(t_w). \tag{17}$$

We are interested in $h \to 0$, but in practical simulations a compromise is needed between this requirement and that of measurability of $\tilde{R}h$. The corresponding correlation function is

$$\tilde{C}(t_w, t + t_w) = N^{-1} \sum_{i=1}^{N} s_i(t_w) s_i(t_w + t) \tag{18}$$

which differs from (4) by the normalization which was introduced into the latter in order to ensure $C(t_w, t_w) = 1$, as is the case for $C(0)$ for conventional correlation functions used in spin and structural glass theory; it is needed for C in this case because the magnitude of $\sum_i s_i^2(t)$ is not conserved in our problem.

In order to maintain the feature $C(t_w, t_w) = 1$ we normalize $\tilde{C}$ and $\tilde{R}$ also for these non-equilibrium studies, with interesting differences depending on the choice. Thus we consider (i) normalization by $e(t + t_w) = N^{-1} \sum_i s_i^2(t + t_w)$ which we shall indicate by a subscript $t + t_w$, as $C_{t+t_w}(t_w, t + t_w)$, and (ii) normalization by $e(t_w)$, denoted by a subscript t_w. Note that in equilibrium $e(t_w) = e(t + t_w)$ but this is not true out of equilibrium. For FDT investigation the former normalization is appropriate, but the latter is also instructive.

Figures 8(a) and (b) show results of parametric plots for C_{t_w} and C_{t_w+t} for the hexagonal lattice with $D > 0$. The first shows deviations from slope -1 while the latter has the usual -1 slope of a system obeying FDT. More particularly, figure 8(a) shows first deviations to a slope less steep than -1, as reminiscent of what is found for a fragile glass, but then behaves non-monotonically (note that conventionally one reads these curves from right to left). The non-monotonicity is a result of the competition between the applied field, which encourages non-zero spins to settle on favourable sites and thus increase the response, and the natural relaxation to equilibrium, which removes non-zero spins altogether thus reducing the response. Without figure 8(b) one might be led to think this represents breaking of FDT. The actual situation is made clearer by the plots of C and $(1 - R)$ against time, given in figure 8(c), which are clearly superimposed as required by FDT but also each have interesting t-dependence due to defect annihilation.

In contrast there is evidence for FDT breaking in the case $D < 0$, presumably due to the blockades consequential to the ± 1 ground states, as mentioned briefly above. For further details, however, the reader is referred to [7]. Here we restrict ourselves to the observation that our results indicate that great caution must be exercised in avoiding over-naive interpretation of correlation–response plots to deduce FDT breaking.

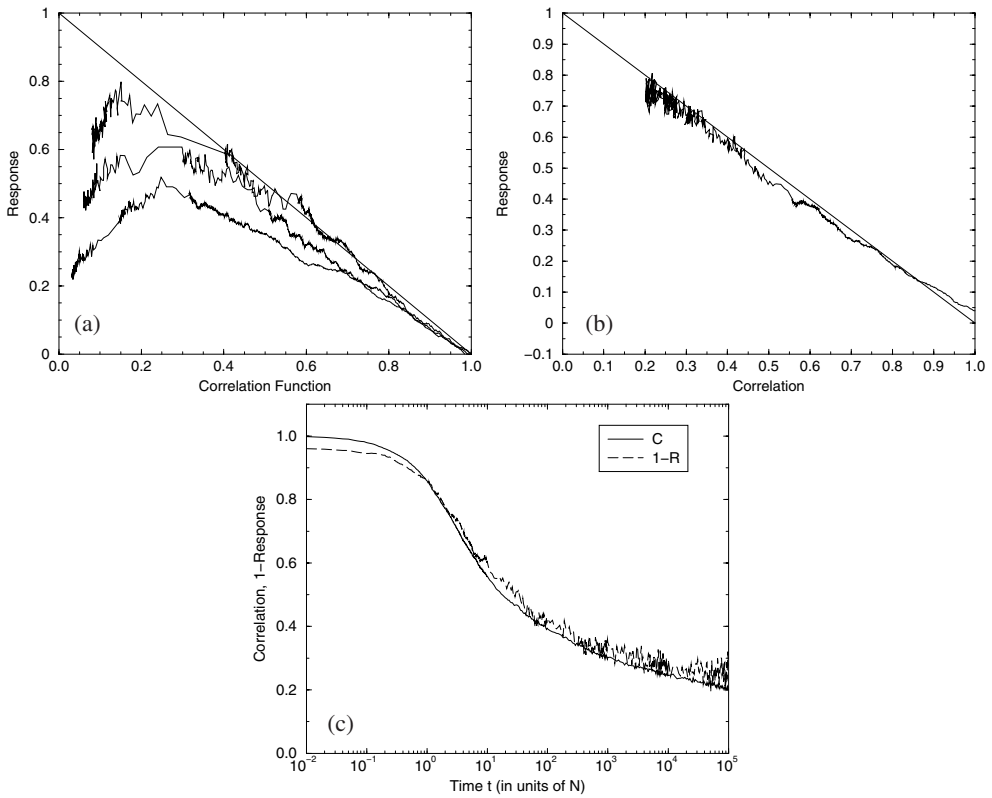

Figure 8. Hexagonal system with $D > 0$. (a) Response R_{t_w} versus $C_{t_w}(t_w, t_w + t)$ for $\beta = 4$ and $t_w = 10$ N, 10^2 N, 10^3 N (from the lower to upper curve). (b) Response R_{t_w+t} versus $C_{t_w+t}(t_w, t_w + t)$ for $\beta = 7$, $t_w = 10^2$ N. The straight lines of slope -1 are shown for comparison. (c) $C_{t_w+t}(t_w, t_w + t)$ and $(1 - R_{t_w+t})$ as functions of t for $\beta = 7$, $t_w = 10^2$ N.

5. Conclusion

By means of study of a series of simple models we have demonstrated how constrained dynamics of an appropriate type suffices to yield energy and autocorrelation evolution behaviour qualitatively analogous to that found in real glasses. We have provided a simple interpretation in terms of annihilation–diffusion processes of two timescales, one temperature independent, the other Arrhenius. On the other hand the fluctuation-dissipation relation is not broken if one chooses the correct normalizations, although with the wrong normalization it might appear to be broken.

Our current studies are appropriate to a mimicking of strong glasses, complementary to studies of fragile glasses, but might be extended.

Acknowledgments

The authors would like to thank T Aste, J Cardy, F Ritort, E Moro and S Krishnamurthy for helpful discussions. LD, DS and JPG acknowledge financial support from EPSRC (grant GR/M04426 and studentship 98311155), AB from EU (Marie Curie HPMF-CT-1999-00328), and JPG from a Glasstone Research Fellowship (Oxford). Parts of this work were first reported at a workshop within the ESF SPHINX programme.

References

[1] Angell C A 1995 *Science* **267** 1924
[2] Aste T and Sherrington D 1999 *J. Phys. A: Math. Gen.* **32** 7049
[3] Davison L and Sherrington D 2000 *J. Phys. A: Math. Gen.* **33** 8615
[4] Davison L, Sherrington D, Garrahan J P and Buhot A 2001 *J. Phys. A: Math. Gen.* **34** 5147
[5] Cardy J 1999 Field theory and non-equilibrium statistical mechanics *Lectures Presented at the Troisieme Cycle de la Suisse Romande*
[6] Hinrichson H 2000 *Adv. Phys.* **49** 815
[7] Davison L 2001 *D Phil Thesis* University of Oxford